

**NORSAND:  
DESCRIPTION, CALIBRATION, VALIDATION AND  
APPLICATIONS**

Dawn Shuttle & Michael Jefferies

June 2010

## SCOPE OF DOCUMENT

This document is a reference text for engineers wanting to use the *NorSand-M* FISH function available on Itasca's download web site. The “-M” in the model name is used to indicate that this is the version of NorSand for monotonically increasing deviator or mean stress load paths (which includes elastic unloading and reloading). The more advanced aspects of NorSand, including yield in unloading and principal stress rotation, have not yet been ported to FISH.

The situations in which this FISH model implementation may be applicable are outlined, before describing main features of the constitutive model itself. As NorSand has been widely documented in the literature, the reader is also directed to relevant papers providing more detailed explanation of the model and its applications.

How to obtain input parameters for the model is described in detail – as NorSand, like all constitutive models, only provides useful output with sensible inputs. Generally, both laboratory and in situ testing is needed and these aspects are discussed. Some example parameters sets from a range of soil types are given.

Finally, a short description of the two example files downloadable from the Itasca download web site is given.

## NOTATION

### Stress Variables

$\sigma_{1,2,3}$	[FL <sup>-2</sup> ]	Principal stresses, bar superscript denoting effective
$\bar{\sigma}_m$	[FL <sup>-2</sup> ]	Mean effective stress (= $p'$ under triaxial conditions) $\bar{\sigma}_m = (\bar{\sigma}_1 + \bar{\sigma}_2 + \bar{\sigma}_3) / 3$
$\bar{\sigma}_q$	[FL <sup>-2</sup> ]	Deviatoric stress invariant (= $q$ under triaxial conditions) $\bar{\sigma}_q = (\frac{1}{2}(\sigma_1 - \sigma_2)^2 + \frac{1}{2}(\sigma_2 - \sigma_3)^2 + \frac{1}{2}(\sigma_3 - \sigma_1)^2)^{1/2}$
$\eta$	[-]	Dimensionless shear measure as ratio of stress invariants $\eta = \bar{\sigma}_q / \bar{\sigma}_m$
$\theta$	[Rad]	Lode angle, $\sin(3\theta) = -13.5 \bar{\sigma}_1 \bar{\sigma}_2 \bar{\sigma}_3 / \bar{\sigma}_q^3$

### Strain Variables (dot superscript denotes rate)

$e$	[-]	Void ratio
$\varepsilon_{1,2,3}$	[-]	Principal strains (assumed coaxial with principal stresses)
$\varepsilon_v$	[-]	Volumetric strain $\varepsilon_v = \varepsilon_1 + \varepsilon_2 + \varepsilon_3$
$\dot{\varepsilon}_v$	[-]	Volumetric strain rate $\dot{\varepsilon}_v = \dot{\varepsilon}_1 + \dot{\varepsilon}_2 + \dot{\varepsilon}_3$
$\varepsilon_q$	[-]	Shear strain invariant (work conjugate with $\bar{\sigma}_q$ ) $\varepsilon_q = \frac{1}{3}((\sin \theta + \sqrt{3} \cos \theta)\varepsilon_1 - 2 \sin \theta \varepsilon_2 + (\sin \theta - \sqrt{3} \cos \theta)\varepsilon_3)$
$\dot{\varepsilon}_q$	[-]	Shear strain rate (work conjugate with $\bar{\sigma}_q$ ) $\dot{\varepsilon}_q = \frac{1}{3}((\sin \theta + \sqrt{3} \cos \theta)\dot{\varepsilon}_1 - 2 \sin \theta \dot{\varepsilon}_2 + (\sin \theta - \sqrt{3} \cos \theta)\dot{\varepsilon}_3)$
$D^p$	[-]	Plastic dilatancy, $\dot{\varepsilon}_v^p / \dot{\varepsilon}_q^p$ (note defined on rates)

### Variables & Parameters

$G$	[FL <sup>-2</sup> ]	Shear modulus, a model parameter
$H$	[-]	Plastic hardening modulus, a model parameter
$I_r$	[-]	Soil rigidity, $G / \bar{\sigma}_m$
$K_0$		Geostatic stress ratio, $\bar{\sigma}_v / \bar{\sigma}_h$
$M$	[-]	Critical friction ratio, a model parameter
$N$	[-]	Volumetric coupling coefficient, a model parameter
$Q$	[-]	Dimensionless CPT tip resistance, $Q = (q_t - \sigma_v) / \bar{\sigma}_v$
$q_t$	[FL <sup>-2</sup> ]	CPT tip resistance
$R$	[-]	Over-consolidation measure, representing proximity of state point to its yield surface
$\nu$	[-]	Elastic Poisson's ratio, a model parameter and usually constant
$\chi$	[-]	Dilatancy constant, a model parameter
$\phi$	[Rad]	Mohr Coulomb friction angle
$\Gamma$	[-]	Reference void ratio on CSL, a model parameter
$\lambda$	[-]	Slope of CSL in $e$ - $\ln(\sigma_m)$ space, a model parameter
$\kappa$	[-]	Slope of elastic line in $e$ - $\ln(\sigma_m)$ space
$\psi$	[-]	State parameter, $\psi = e - e_c$

*Subscripts*

<i>c</i>	Critical state
<i>h</i>	Horizontal
<i>i</i>	Image condition on yield surface
<i>L</i>	Limit value
<i>tc</i>	Triaxial compression condition ( $\theta = \pi/6$ )
<i>te</i>	Triaxial extension condition ( $\theta = -\pi/6$ )
<i>v</i>	Vertical

## TABLE OF CONTENTS

	Page
1. INTRODUCTION	1
1.1 Why use NorSand ?	1
1.2 Critical State Soil Mechanics	1
1.3 Soil types suitable for NorSand	2
1.4 Applications suitable for <i>NorSand-M</i> FISH Version 6	2
1.5 Sign convention	3
2. OVERVIEW OF NORSAND	4
2.1 Idealizations	4
2.2 Model Description	5
2.3 Parameters and Soil Properties	9
2.4 Validation References	11
2.5 Further Reading	11
3. PROCEDURES FOR CALIBRATION OF NORSAND	13
3.1 Critical state parameters, $\Gamma$ and $\lambda$	13
3.2 Elasticity, $G$ and $\nu$	14
3.3 Plasticity, $M_{tc}$ , $N$ , $\chi$ and $H$	14
3.4 Measuring state	18
3.5 Testing range	22
4. FISH EXAMPLES	24
4.1 Plane strain element test	24
4.2 Passive wall	27
5. REFERENCES	29

## LIST OF FIGURES

	Page
Figure 2-1 Definition of state parameter $\psi$ and overconsolidation ratio $R$	5
Figure 2-2 Illustration of NorSand yield surfaces and limiting stress	8
Figure 2-3 Sand dilatancy at peak strength, $D_{\min}$ , in drained triaxial compression as a function of the state parameter, $\psi$	10
Figure 2-4 Trend in plastic hardening modulus with $\psi$ for Erksak sand	10
Figure 3-1 Example of CSL Determination	14
Figure 3-2 Example of a plotted stress-dilatancy ( $\eta - D$ ) data	15
Figure 3-3 Determination of $M_{tc}$ and $N$ from stress-dilatancy data	16
Figure 3-4 Determination of $\chi$ from a plot of $D^P$ versus $\psi$	16
Figure 3-5 Example triaxial calibration to determine $H$	18
Figure 3-6 Comparison of CPT resistance in Ticino Sand with trendlines from numerical simulations using finite element implementation of NorSand	21
Figure 4-1 Geometry, boundary and loading conditions for Plane.dat	24
Figure 4-2 Results from plane.dat compared against the direct integration VBA solution	26
Figure 4-3 Mesh used for passive wall	27
Figure 4-4 Effect of initial state on the lateral force of a 2m high rough wall	28

## LIST OF TABLES

	Page
Table 2-1 Summary of <i>NorSand-M</i> implemented in FISH V6	6
Table 2-2 NorSand Soil Properties with Typical Range for Sands	9
Table 2-3 Published NorSand Applications	12
Table 3-1 Approximate expressions for general inverse form $\psi=f(Q)$	20
Table 3-2 Some Examples of Calibrated Soil Property Sets for NorSand	23
Table 4-1 NorSand Soil Properties for Example 'Plane'	24
Table 4-2 Tracked outputs for Plane.dat	25
Table 4-3 NorSand Soil Properties for Example 'Rough Wall'	27
Table 4-4 Tracked outputs for the rough wall	28

# 1. INTRODUCTION

## 1.1 Why use NorSand ?

Outside of academia, finite element or FLAC models are typically only used for “non-routine” projects. Even in such non-routine applications the constitutive model is rarely more advanced than Non-Associated Mohr-Coulomb (as even a casual survey of the user manuals for the various commercial codes will indicate). The additional effort in the parameter determination for any advanced constitutive model is only justified for situations where accurate representation of volume changes is important to the overall behaviour of the structure. These situations include problems involving large strain, confinement, or excess pore pressure generation. *NorSand* has been used for a variety of such applications.

An attribute of NorSand is not that it can be used for advanced modelling, but that it is easily used by practical geotechnical engineers. NorSand has few parameters, most of which are familiar. The unfamiliar parameters are easily understood and measured. It really does not need much more effort than a Mohr Coulomb model.

## 1.2 Critical State Soil Mechanics

A striking feature of soil is that it exists over a range of void ratio and the actual void ratio (or density) affects the soil’s constitutive behaviour. A proper constitutive model for soil must explain the changes in soil behaviour caused by changes in its void ratio. One framework that incorporates this density dependence is *Critical State Soil Mechanics* (CSSM) with its most famous model Cam Clay (Schofield & Wroth, 1968), in the form of its derivative Modified Cam Clay (Roscoe & Burland, 1968) arguably the most widely available model for soil in commercial software packages. A kernel of CSSM is the critical state locus (CSL), which is simply the relationship between mean effective stress and critical void ratio. The CSL defines the end condition of all loading paths, and is a delightful (and accurate) mathematical idealization for constitutive modelling of soils.

Although critical state models explain the effect of void ratio on soil behaviour, and they have had some notable successes as in, for example, explaining the effect of over-consolidation on clay strength, critical state models fell out of favour. The basic problem is neither Cam Clay, nor the various variants of Modified Cam Clay, dilate anything like actual dense soils. And dense soils, whether over-consolidated clays or sands, are materials of much practical interest for engineered construction. These original critical state models also poorly predict the behaviour of loose sands, and liquefaction-related behaviours in particular.

NorSand was the first CSSM developed for sand and originated from observations about sand behaviour in large scale hydraulic fills. However, as in many things to do with soil, there were earlier insights - Parry’s (1956) observation that maximum dilatancy scaled with distance from the critical state was key, implemented in NorSand by scaling dilatancy to the *state parameter* ( $\psi$ ). Although ‘sand’ is included in the model name, this was only to differentiate the model from the Cam Clay variants and emphasize the proper modelling of dilatancy – in actuality, NorSand is a plasticity model applicable to any soil in which particle to particle interactions are controlled by contact forces and slips rather than bonds. The classic Cam Clay models can be simulated as special cases of NorSand by appropriate choice of material properties and initial conditions. Although a single name, NorSand, is used the

model has seen progressive enhancement and modification. The version here, *NorSand-M*, is for monotonically increasing deviator or mean stress load paths (which includes elastic unloading and reloading) indicated by the “-M” in the model name. *NorSand-M* in FISH is current to May 2010, with no changes/updates anticipated (this version has been stable for some three years). The more general aspects of NorSand, including yield in unloading and principal stress rotation, have not yet been ported to FISH.

### 1.3 Soil types suitable for NorSand

NorSand has been applied to a range of soils from clayey silt to sand with good success. Initially NorSand was primarily used for modelling sand behaviour, and enough experience now exists with NorSand to provide typical parameter ranges for sand (e.g. Table 2-2). More recently NorSand has been applied to a range of projects where the soil of interest was silt, and with equally good results. But when modelling silt extra care should be taken in the assignment of material properties as the ‘typical’ range of values for sand may not apply. For example, recent testing of silt tailings in the laboratory has shown very high values of critical state strength ratio,  $M$ . And the value of the dilatancy parameter  $\chi_{tc}$  may also diverge from the usual sand range.

To date, NorSand has not been used to model clay behaviour. But in principle there is no reason that the model could not be applied to model the strength behaviour of any uncemented soil, including clay.

### 1.4 Applications suitable for *NorSand-M* FISH Version 6

Critical state type models represent the effect of void ratio on a soil’s behaviour. That is, using a single set of material properties, the differing stress-strain behaviour caused by differing initial void ratios is computed (and regardless of stress level). Given this background, it is unsurprising that one of the first applications of *NorSand-M* was to understand the cone penetration test (CPT). This work was then extended to the pressuremeter. Both tests are situations where interest focuses on the in situ void ratio, and where there is substantial confinement that magnifies the effect of dilatancy – to date, only critical state models have captured the details of the complex conditions around these important in situ tests. Given the success with in situ test evaluation, a reasonable application of *NorSand-M* would be soil anchors/nails and reinforced earth in particular; research work is underway on applying NorSand to reinforced earth.

Ground improvement is a natural application for critical state models since the intent of much of this type of work is to increase the soils density. *NorSand-M* has been used extensively in engineering compaction grouting and features in the new ASCE (2010) guide for this method of ground improvement.

Although confinement magnifies the effect of dilation, by properly accounting for stress-dilatancy and plastic hardening *NorSand-M* accurately models the evolution of soil stiffness without resorting to a ‘strain dependent modulus’. The implemented FISH is therefore applicable to modelling of soil-structure interaction (first loading). It has been validated in this role for horizontal loading of a large offshore platform by 2m thick moving sea ice (publications pending).

Soil liquefaction has been a major topic of interest to geotechnical engineering for the past three decades or so. Indeed, the state parameter developed out of work in just this context. The realistic evolution of plastic strains makes NorSand suitable for undrained, as well as drained, situations. Liquefaction comes in broadly two situations: cyclic mobility and/or static failures. Modelling cyclic mobility requires NorSand-PSR (where PSR denotes principal stress rotation). However, static liquefaction is well within the capability of *NorSand-M*, whether for purely undrained situations or in a coupled ‘Biot’ type analysis with internal migration of pore water.

The complete NorSand-PSR constitutive model includes principal stress rotation and yield in unloading, and hence can represent both cyclic loading and the effect of loading-unloading cycles during construction. The authors intend to add this additional model capability in future versions of the FISH.

## **1.5 Sign convention**

In what follows a compression positive convention is adopted, with the bar notation " - " denoting effective stress. This sign convention follows the original published derivations, and is adopted within the FISH, but differs from the general sign convention within FLAC. Most of the notation used is standard and a complete list of notation is given in the preceding *Notation* section.

## 2. OVERVIEW OF NORSAND

This section provides an overview of NorSand and its applicability for general engineering problems.

### 2.1 Idealizations

Critical state soil mechanics is based on two ideas, often unstated, but which define the framework: (1) a unique critical state locus (CSL) exists; (2) soils move to the CSL with shear strain.

NorSand is also an idealized critical state model and with four further ideas:

- There are an infinity of possible yield surfaces in  $e - \bar{\sigma}_m$  space such that any yield surface does not necessarily intersect the CSL, with the position of the current yield surface in the  $e - \bar{\sigma}_m$  space being defined by  $\psi$
- The state parameter  $\psi$  tends to zero (intersection of the yield surface with the CSL) as shear strain accumulates
- The minimum possible dilation rate (i.e. dilation at peak strength) is linearly related to  $\psi$
- Principal stress rotation always softens (shrinks) the yield surface

The state parameter  $\psi$  is a measure of the current void ratio relative to the critical state void ratio at the same mean effective stress.

$$\psi = e - e_c \quad (1)$$

...where  $e$  is the actual void ratio of the soil and  $e_c$  is the critical void ratio of that soil at the current mean stress. In essence,  $\psi$  represents whether the soil will want to dilate or contract as it is sheared towards failure, and by how much.

Data gathered on a wide range of sand indicates that an infinity of normal compression lines (NCL) exist, rather than the single NCL assumed in the Cam Clay soil model. This infinity of NCL forces two parameters to characterize the state of a soil:  $\psi$  and  $R$ . The state parameter  $\psi$  is a measure of the location of an individual NCL in  $e - \bar{\sigma}_m$  state space, which is the second idea above. The over-consolidation ratio  $R$  represents the proximity of a state point to its yield surface when measured along the mean effective stress axis. The variable  $\bar{\sigma}_{m,\max}$  is the equivalent maximum mean effective stress experienced by the soil, which might be thought of as a pre-consolidation pressure (although that term is commonly applied in the sense of vertical effective stress). Note in particular that  $R$  and  $\psi$  are not alternate identities as is implied by Cam Clay or its variants;  $R$  and  $\psi$  represent measures of different things as illustrated on Figure 2-1.

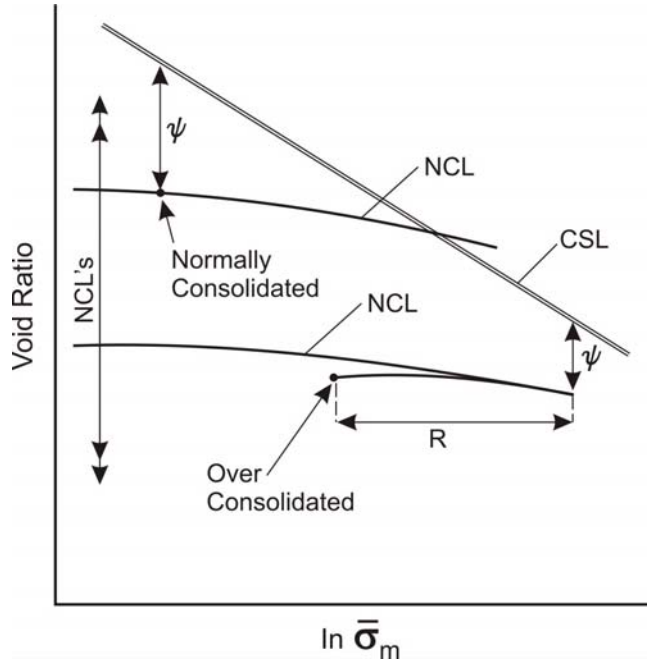


Figure 2-1 Definition of state parameter  $\psi$  and overconsolidation ratio  $R$

Because NorSand (like the Cam Clay variants) idealizes plastic work dissipation it is essential to use work conjugate stress and strain measures for self-consistency of the model. This requires a different deviatoric strain invariant from that commonly used in numerical analysis:

$$\varepsilon_q = \frac{1}{3} \left( (\sin \theta + \sqrt{3} \cos \theta) \varepsilon_1 - 2 \sin \theta \varepsilon_2 + (\sin \theta - \sqrt{3} \cos \theta) \varepsilon_3 \right) \quad (2)$$

Because Lode angle typically varies during a simulation, Equation (2) is often defined as the increment of deviatoric strain invariant,  $\dot{\varepsilon}_q$ , using incremental strains and the current Lode angle. Equation (2) is also linear, allowing decomposition of strain into elastic and plastic components within the invariant. Although uncommon, this strain invariant is some twenty years old having been first suggested by Resende & Martin (1985).

## 2.2 Model Description

The critical state, which is the condition at which soils deform continuously and indefinitely at constant volume, is used as the reference framework. The void ratio of the critical state  $e_c$  depends on the mean effective stress  $\bar{\sigma}_m$ , and various relations have been proposed for this. These different relations are details, and preference for one relation over another to fit the behaviour of a particular soil is only an issue for calibration as the basic framework of NorSand is unchanged. For many purposes the familiar  $e_c = \Gamma - \lambda \ln(\bar{\sigma}_m)$  idealization is both simple and sufficiently accurate, and is implemented in the FISH.

The critical state is also a relationship between mean and shear stress, and this has been extensively investigated. To a high precision and high stress levels, the critical state is fitted by  $\bar{\sigma}_{q,c} = M \bar{\sigma}_{m,c}$  (where the subscript 'c' denotes critical conditions and  $M$  is a soil property). More precisely,  $M$  varies with the proportion of intermediate principal stress (usually given as

the Lode angle) and the soil property is conventionally defined under triaxial compression conditions as  $M_{tc}$  with the subscript 'tc' being used to indicate this. Although the variation in peak strength with Lode angle has been investigated for several soils, there has been far less investigation of  $M$  itself.

NorSand is a plasticity model for soil. As such, and in common with other plasticity models, it comprises three items: (1) a yield surface; (2) a flow rule; and, (3) a hardening law. These three aspects of the NorSand model are described below, with the equations of the model equations summarized on Table 2-1. Note that Table 2-1 describes the *NorSand-M* model implemented in the NorSand FISH V6 function. Some aspects of NorSand, including the internal cap and cyclic softening, have not been incorporated into the FISH function. It is intended that these will be included in the .dll version of the NorSand routine.

Table 2-1 Summary of *NorSand-M* implemented in FISH V6

Internal Model Variables	$\psi_i = \psi + \lambda \ln(\bar{\sigma}_{m,i} / \bar{\sigma}_m) \quad \text{where } \psi = e - e_c$ $M_i = M \left( 1 - \frac{N\chi \psi }{M_{tc}} \right)$
Critical State	$e_c = \Gamma - \lambda \ln(\bar{\sigma}_m) \quad \text{AND} \quad \eta_c = M$ <p>where <math display="block">M = M_{tc} - \frac{M_{tc}^2}{3 + M_{tc}} \cos(3\theta/2 + \pi/4)</math></p>
Yield Surface & Internal Cap	$\frac{\eta}{M_i} = 1 - \ln\left(\frac{\bar{\sigma}_m}{\bar{\sigma}_{m,i}}\right) \quad \text{with} \quad \left(\frac{\bar{\sigma}_{m,i}}{\bar{\sigma}_m}\right)_{\max} = \exp(-\chi_{tc}\psi_i/M_{i,tc})$
Hardening Rule	<p>On outer yield surface:</p> $\frac{\dot{\bar{\sigma}}_{m,i}}{\bar{\sigma}_{m,i}} = H \frac{M_i}{M_{i,tc}} \left(\frac{\bar{\sigma}_m}{\bar{\sigma}_{m,i}}\right)^2 \left[ \left(\frac{\bar{\sigma}_{m,i}}{\bar{\sigma}_m}\right)_{\max} - \frac{\bar{\sigma}_{m,i}}{\bar{\sigma}_m} \right] \dot{\chi}_q^p$
Stress Dilatancy & Plastic Strain Rate Ratios	$D^p = \dot{\chi}_q^p / \left  \dot{\chi}_q^p \right  M_i - \eta \Rightarrow D_{tc}^p = D^p M_{i,tc} / M_i \quad \text{and} \quad D_{te}^p = D^p M_{i,te} / M_i$ <p>define <math display="block">\xi_{3,tc} = \frac{2D_{tc}^p - 3}{6 + 2D_{tc}^p} \quad \text{and} \quad \xi_{3,te} = \frac{2D_{te}^p - 6}{3 + 2D_{te}^p}</math></p> $\Rightarrow \frac{\dot{\epsilon}_3}{\dot{\epsilon}_1} = \xi_{3,tc} - (\xi_{3,tc} - \xi_{3,te}) \cos\left(\frac{3\theta + 90}{2}\right)$ <p>define <math display="block">a = (\sin\theta + \sqrt{3}\cos\theta)/3, \quad b = -2\sin\theta/3,</math></p> $c = (\sin\theta - \sqrt{3}\cos\theta)/3$ $\Rightarrow \frac{\dot{\epsilon}_2}{\dot{\epsilon}_1} = (aD^p - 1 + \frac{\dot{\epsilon}_3}{\dot{\epsilon}_1}(cD^p - 1))/(1 - bD^p)$
Elasticity	<p>G with <math display="block">K = \frac{2(1+\nu)}{3(1-2\nu)} G</math></p>

In Table 2-1 note that Jefferies & Shuttle (2002) suggested that  $M$  be taken as an average of the Mohr-Coulomb and Matsuoka & Nakai (1974) criteria. This approximation, although adequate, had the disadvantage that the Matsuoka & Nakai criteria needed to be solved numerically – and which was extremely inefficient for implementation within FISH. The updated expression for  $M$  (see Jefferies & Shuttle, 2010) is both more accurate and numerically simple to implement.

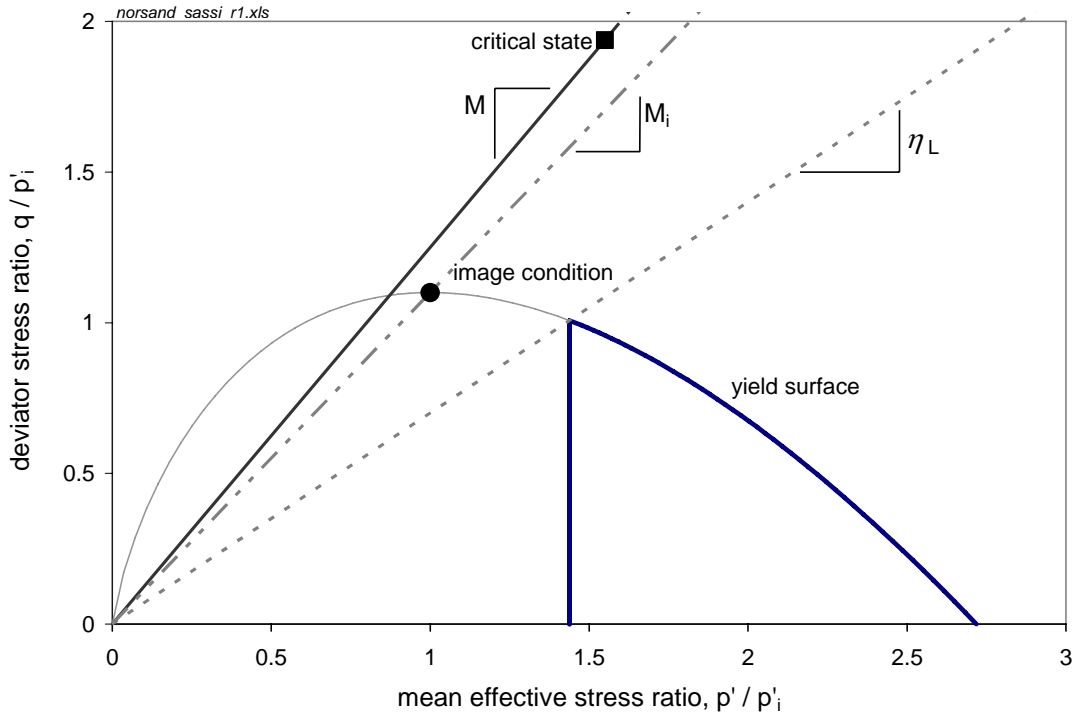
The NorSand yield surface has the familiar bullet-like shape of the classical Cam Clay model but with one important addition – a limit is invoked to prevent unrealistically large dilation of dense soils.

The plastic dilatancy  $D^p$  is determined from the idealized stress-dilatancy relation that underlies the model, but as there are three strain rates this is insufficient to determine each of them. The intermediate principal strain rate is therefore interpolated depending on the Lode angle. This interpolation approach is somewhat unusual for plasticity models, but is taken to ensure consistency with the work dissipation postulate that is the basis of the model.

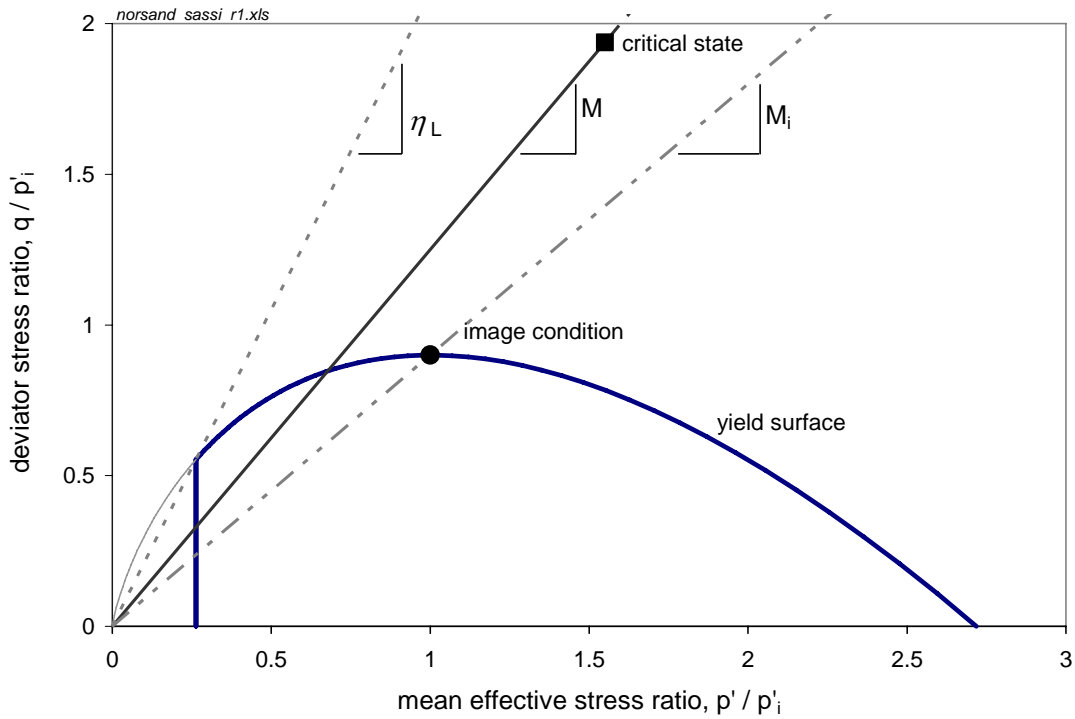
The third aspect of the model is the hardening law, which describes how the yield surface increases or decreases in size with plastic straining. The size of the yield surface is controlled by what is termed the image stress  $\bar{\sigma}_{m,i}$  and which forms the object of the hardening law. It is called the image stress because it represents a situation in which one of the two conditions for the critical state is met, and the meaning is readily apparent from Figure 2-2.

NorSand is an isotropic model hardening which expands or contracts the yield surface, as required by the hardening law, while retaining its shape. The value of the limiting dilation evolves with the changing state parameter. Whether the yield surface hardens or softens depends on two things: the current state parameter; and, the direction of loading. Loading past the internal cap always softens the yield surface. However, the key determinant in the general hardening is the state parameter. As illustrated on Figure 2-2, the critical state does not usually intersect the yield surface (this is the largest single difference between NorSand and Cam Clay). This divergence of yield surface from critical state is used as the basis of the hardening law, and the hardening law acts to move the yield surface towards the critical state under the action of plastic shear strain – which directly captures the essence of critical state principles.

Elasticity in soils is arguably a more complicated aspect than plasticity. However, for most situations involving soil modelling this sophistication is unwarranted. On one hand the soil fabric (grain arrangement) substantially affects modulus and thus elastic modulus should be measured in situ. On the other hand, plastic strains often dominate. For most purposes constant shear rigidity,  $I_r (= G / \bar{\sigma}_m)$  and constant Poisson's ratio,  $\nu$ , is a sufficient representation of elasticity. The NorSand FISH reads shear modulus,  $G$ , and Poisson's ratio,  $\nu$ .



(a) Very loose sand



(b) Very dense sand

Figure 2-2 Illustration of NorSand yield surfaces and limiting stress

## 2.3 Parameters and Soil Properties

*NorSand-M* is a sparse model. For the CSL approximated as a semi-log form, and with the simplest representation of elasticity, there are eight model properties. These properties are summarized on Table 2-2 with typical ranges in values for sands indicated. How to determine these soil properties is presented in Section 3 after the model performance has been illustrated, and examples of calibrated parameter sets are given then. Seven of the properties are dimensionless, although  $\Gamma$  has a reference stress level associated with it. Most of the parameters are familiar including  $\Gamma$ ,  $\lambda$ ,  $M_{tc}$ ,  $G$  and  $\nu$  and as such require no further comment. Only three parameters may be unfamiliar.

The parameter  $N$  is a volumetric coupling parameter, and is defined in the same way as the parameter  $N$  found in Nova's flow rule (Nova, 1982). The value of  $N$  does not vary greatly, and in earlier versions of *NorSand* the parameter,  $N$ , was often assumed to be 0.3 for simplicity. However, this parameter is simple to obtain from a few triaxial compression tests and has been reintroduced to improve model accuracy.

The parameter  $\chi_{tc}$  is the slope of the trend line for minimum dilatancy in Figure 2-3. In the original version of *NorSand* this trend was thought to be a model constant. But, further data has shown that  $\chi_{tc}$  varies somewhat from soil to soil and could also be a function of soil fabric. The reference condition is taken as triaxial compression because dilatancy is itself a function of Lode angle.

The plastic hardening modulus  $H$  can in principle be a function of soil fabric, and data to date suggests that it is also a function of  $\psi$ . Figure 2-4 shows some data illustrating these aspects. There is some evidence that  $H$  is proportional to  $1/(\lambda-\kappa)$  and which is what might be anticipated from analogy to Cam Clay. On the other hand, such a linkage should also be anticipated to be affected by soil fabric.

Table 2-2 *NorSand* Soil Properties with Typical Range for Sands

<b><i>Property</i></b>	<b><i>Typical Range</i></b>	<b><i>Remark</i></b>
<i>CSL</i>		
$\Gamma$	0.9 – 1.4	'Altitude' of CSL, defined at 1 kPa
$\lambda$	0.01 – 0.07	Slope of CSL, defined on base e
<i>Plasticity</i>		
$M_{tc}$	1.2 – 1.5	Critical friction ratio, triaxial compression as reference condition
$N$	0.2 - 0.45	Volumetric coupling coefficient
$H$	50 – 500	Plastic hardening modulus for loading, often $f(\psi)$
$\chi_{tc}$	2.5 – 4.5	Relates minimum dilatancy to $\psi$ . Often taken as 3.5. Triaxial compression as reference condition
<i>Elasticity</i>		
$I_r$	100-800	Dimensionless shear rigidity
$\nu$	0.1 – 0.3	Poisson's ratio, commonly 0.2 adopted

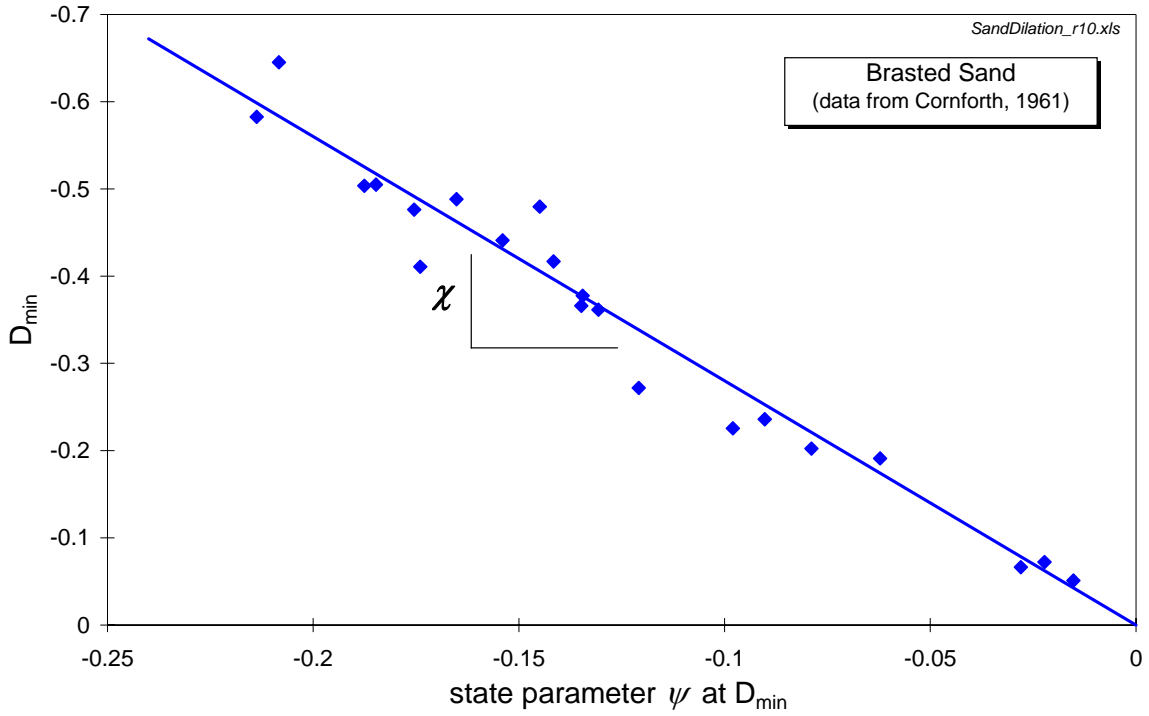


Figure 2-3 Sand dilatancy at peak strength,  $D_{min}$ , in drained triaxial compression as a function of the state parameter,  $\psi$

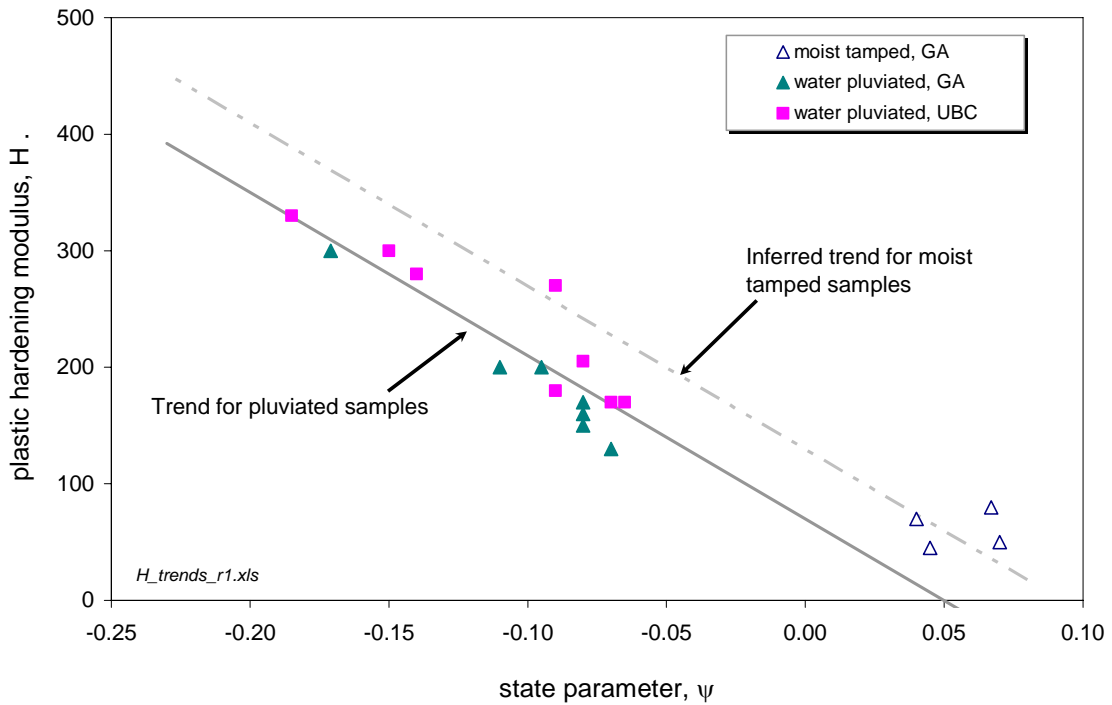


Figure 2-4 Trend in plastic hardening modulus with  $\psi$  for Erksak sand

There is less experience at applying NorSand to silts and clays, with much work in this area being recent. What can be noted is that with well-graded sandy silts the dilatancy parameter  $\chi_{tc}$  takes much greater values, presumed to be a consequence of less void ratio space between  $e_c$  and  $e_{min}$  with such soils.  $H$  seemingly scales with  $1/(\lambda-\kappa)$  as noted earlier.

## 2.4 Validation References

An unusual aspect of the NorSand constitutive model is that a significant number of comparisons between NorSand and laboratory data have been published in the literature. And because NorSand is calibrated under triaxial conditions, simulations for stress paths other than triaxial compression (e.g. plane strain, cyclic simple shear) provide a validation of the model in general 3-D stress space.

The listing of NorSand literature, provided in Section 2.5, includes a range of papers describing NorSand validation over a range of stress conditions. But for the reader interested in this topic the following three references are recommended.

- (i) Jefferies & Shuttle (2002). This article is recommended because it documents the validation of NorSand under the most widely used 2-D approximation of field conditions, and the default strain condition for FLAC, plane strain. Any model used for 'real' engineering should be validated in plane strain.

The technical note by Jefferies & Shuttle (2010) updates the function used to describe the variation of mobilized shear strength with Lode angle. The new function is more accurate and also markedly more efficient numerically.

- (ii) Jefferies & Shuttle (2005) is a good general read. The authors were allowed additional space (33 pages) to provide an overview of the NorSand model and examples of NorSand validation for a range of stress paths. Validation examples include static liquefaction, with and without static bias – behaviours of practical importance in seismic regions.
- (iii) Finally, the book by Jefferies and Been (2006) is recommended if you intend to use NorSand on a regular basis. This document provides the most in-depth overview of the NorSand model, in addition to the widest range of validation cases. It also provides an in-depth discussion of the use of the model for practical engineering problems.

It is hoped that readers will make use of these references to run the validation cases for themselves. Much of the validation data is available from the web site associated with "Soil Liquefaction: A critical state approach" (Jefferies & Been, 2006) at [www.golder.com/liq](http://www.golder.com/liq).

## 2.5 Further Reading

NorSand has been well documented in the literature. This document is focused on the aspects of the NorSand model and modelling that directly relate to the posted FISH function. But other capabilities of the model exist. The complete version of NorSand contains yield in unloading and principal stress rotation, making it applicable to cyclic loading in addition to the monotonic loading condition coded in *NorSand-M* V6 FISH.

Table 2-3 contains a compilation of references related to the model and its application respectively with the full citations being given in Section 5). These references are not posted on the Itasca model download site, but the authors' have copies of most of these articles if you have difficulty getting hold of them.

Table 2-3 Published NorSand Applications

<i>Topic</i>	<i>Reference</i>	<i>Comment</i>
NorSand	Jefferies (1993)	Original version of NorSand for triaxial conditions.
	Jefferies (1997)	Yield in unloading
	Jefferies and Been (2000)	Isotropic compression of sand, with data on infinity of NCL's
	Jefferies and Shuttle (2002)	Generalization to 3D with plane strain validation
	Jefferies and Shuttle (2005)	Comprehensive overview of the NorSand model with calibrations
	Dabeet and Shuttle (2008)	Yielding in unloading
FISH	Rousé, Shuttle, and Fannin (2006)	Out of date, but includes a clear summary of overall approach
	Jefferies and Shuttle (2010)	Derivations of current FISH function equations
CPT Interpretation	Shuttle and Jefferies (1998)	General methodology for determination of in situ state.
	Ghafghazi and Shuttle (2008a)	Demonstration of inversion method for sands.
	Ghafghazi and Shuttle (2008b)	Offshore Case history comparing CPT and SBP interpretation
	Shuttle and Cunning (2007)	Case history involving very loose tailings
	Shuttle and Cunning (2008)	Includes liquefaction susceptibility chart based on CPT interpretation
Pressuremeter analysis	Shuttle, D.A. (2003)	Pore pressure dissipation
	Shuttle, D.A. (2006)	Determining fabric from the SBP
	Ghafghazi, M., and D.A. Shuttle (2008b)	Offshore Case history comparing CPT and SBP interpretation
Compaction Grouting	Shuttle and Jefferies (2000)	Repair of sinkholes at Bennett Dam
	Jefferies and Shuttle (2002)	Effect of excess pore pressures on compaction grouting
Pile installation	Vyazmensky et al. (2004)	Pore pressure generation during helical pile installation
	Vyazmensky (2004)	Pore pressure and effective stress changes during and after helical pile installation

### 3. PROCEDURES FOR CALIBRATION OF NORSAND

NorSand, as implemented within *NorSand-M* FISH Version 6, has eight material properties (see Table 2-2). All seven properties may typically be obtained from 5 to 7 standard triaxial compression tests on reconstituted samples.

In addition two measures of state are required for input into the FISH: the state parameter,  $\psi$ , and a measure of over-consolidation,  $R$ . The following text documents the recommended method for determining soil properties, and seeks to highlight more common pitfalls.

#### 3.1 Critical state parameters, $\Gamma$ and $\lambda$

The critical state parameters  $\Gamma$ ,  $\lambda$  are determined using triaxial compression tests on reconstituted samples of loose soil. Reconstituted samples are sufficient as the critical state properties are independent of soil structure. Loose soil is used to ensure completely contractive behaviour, and which then provides a clear indication of the critical state without localization issues. Commonly samples are prepared by moist tamping. Although moist tamping is controversial in some circles due to the potential for non-homogeneous samples, moist tamping produces looser samples than other reconstitution methods and hence makes reaching the critical state within the strain limits of the triaxial test more likely. In all cases testing should use modern triaxial equipment with internal load transducers and digital data acquisitions systems. Bender elements are very helpful, and highly recommended.

Problems with critical state testing often trace to careless measurement of void ratio (Sladen & Handford, 1987), and are easily avoided. After a test triaxial test has been completed, close the drainage lines and put the sample, still on its pedestal, into a freezer (a domestic freezer is perfectly adequate). Once frozen, the sample can be demounted without loss of pore water, and its void ratio accurately determined by simply measuring its water content as the sample will be saturated.

Testing should aim to have two samples tested undrained and two tested drained. A fifth sample is in reserve depending on what is found with the first four. The two loose undrained tests are typically consolidated isotropically to 50 kPa and 500 kPa effective confining stress. Undrained shear will then produce substantially contractive behaviour and lead to a clear determination of the critical state mean effective stress for that sample's void ratio at the start of shear and comfortably within the strain limits of the test equipment. It is inconvenient to ascertain the critical void ratio of denser samples using undrained tests, as the initial cell pressures have to be very large. A simpler approach is to use drained triaxial tests on very loose samples, typically from initial effective confining stresses of 200 kPa and 800 kPa. Such samples will be contractive and reach the critical state within the limits of the triaxial test. Figure 3-1 illustrates some state paths for these procedures on an example soil (a silty sand with 35% silt sized or smaller).

As shown on Figure 3-1, the best-fit straight line on the semi-log plot through the end of test conditions gives the  $\Gamma$  and  $\lambda$  parameters for the soil. Generally this simple representation of the CSL is satisfactory for practical engineering, although a curved line is usually a slightly more accurate representation of the CSL as also indicated on Figure 3-1 (eg Verdugo, 1992).

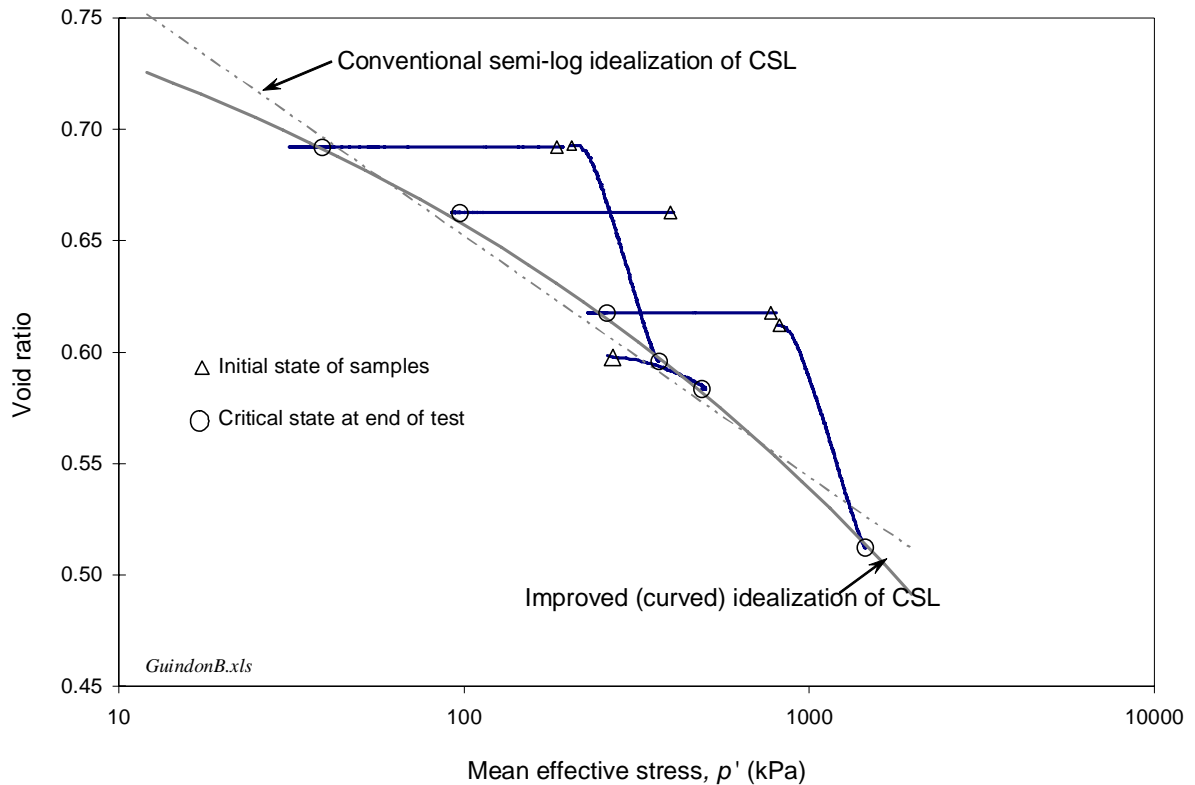


Figure 3-1 Example of CSL Determination

### 3.2 Elasticity, $G$ and $\nu$

The elastic shear modulus is ideally and simply measured using bender elements. Nowadays many commercial laboratories have bender equipment, so it is strongly recommended that benders are used if possible.

In the absence of bender equipment, in principle a sample can be unloaded/reloaded during triaxial shear, but then issues arise on the ability of the triaxial equipment to resolve small strains as well as the effects of yield in unloading (and which thus requires the unload/reload cycle to be markedly before peak strength and of small amplitude).

It is worth noting that elasticity is an important component of soil behaviour. Recent work predicting in situ state from the CPT using NorSand (Ghafghazi & Shuttle, 2008a) found that the accuracy of the model predictions was improved by measuring  $G$  using bender elements. So measure if you can!

Soil behaviour is less sensitive to Poisson's ratio, hence Poisson's ratio is usually not measured but assumed to be in the range 0.1 to 0.2.

### 3.3 Plasticity, $M_{tc}$ , $N$ , $\chi$ and $H$

Historically, the critical state friction ratio,  $M_{tc}$ , was determined from the end of triaxial tests on loose samples (the same tests as used to determine the CSL). While this may still be used, this is no longer the recommended procedure. Using the last data point from very loose triaxial compression tests appears, in some cases, to result in anomalously low values of  $M_{tc}$ .

Instead it is recommended that, where possible, 2 or 3 dense triaxial compression tests are conducted, over a range of pressure. The minimum pressure should be fairly low, say 100 kPa, to provide at least one strongly dilatant dataset. These tests are plotted up as stress ratio ( $\eta = \bar{\sigma}_q / \bar{\sigma}_m$ ) versus dilatancy ( $D = \dot{\epsilon}_v / \dot{\epsilon}_q$ ) as shown in the example on Figure 3-2

(although the  $\eta$  vs.  $D$  plot may not be familiar, it is simple to construct in a spreadsheet such as Excel). Because the value of stress ratio should equal  $M_{tc}$  at the critical state, extrapolation of a straight line through the peaks of these dense tests to  $D = 0$  equals  $M_{tc}$ , as illustrated in Figure 3-3.

Occasionally it has been suggested that a 'short cut' to obtaining  $M_{tc}$  is to use value of stress ratio,  $\eta$ , at  $D = 0$  during loading. This value should not be used, as inspection of Figure 3-2 illustrates. Real sand may (and usually does!) cross the y axis of the  $\eta$ - $D$  plot at a stress ratio below  $M_{tc}$ , resulting in an underestimation of  $M_{tc}$ .

The volumetric coupling parameter,  $N$ , is also ideally determined from Figure 3-3. The slope of the line through the peak of the individual  $\eta$ - $D$  data is  $(1-N)$ . However, for clean sands at least, the value of  $N$  is usually in the range 0.2 to 0.4. Hence a mid-range value of 0.3 is a reasonable estimate in the absence of more detailed data.

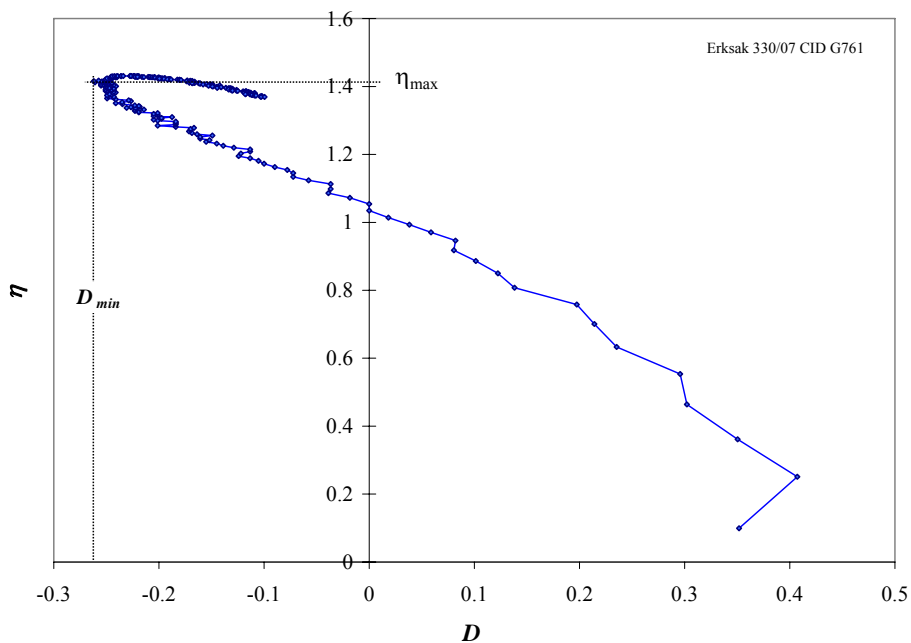


Figure 3-2 Example of a plotted stress-dilatancy ( $\eta$  -  $D$ ) data

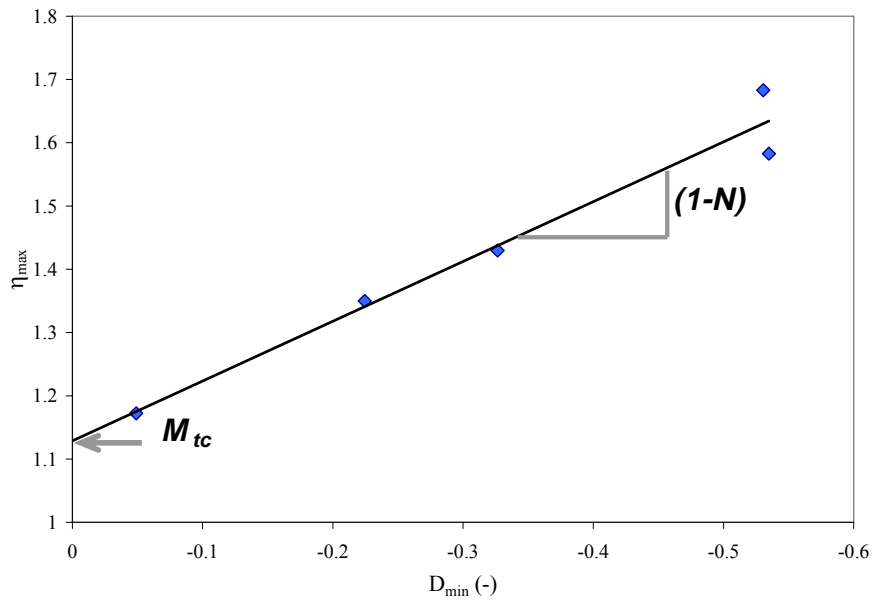


Figure 3-3 Determination of  $M_{tc}$  and  $N$  from stress-dilatancy data

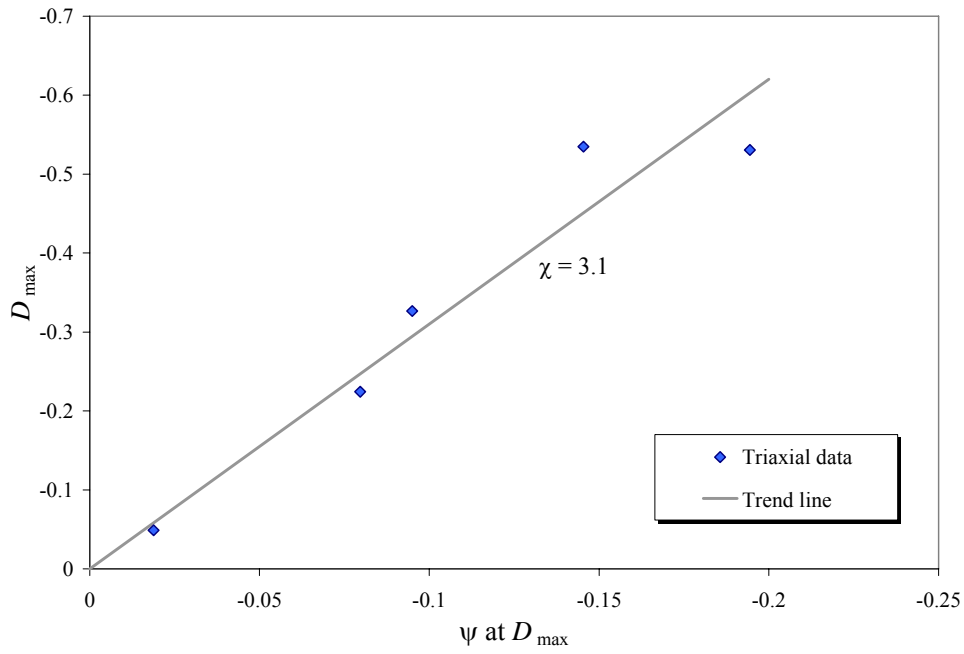


Figure 3-4 Determination of  $\chi$  from a plot of  $D^P$  versus  $\psi$

The dilatancy parameter,  $\chi$ , relates minimum plastic dilatancy to the corresponding state parameter (i.e.  $D^p$  and  $\psi$ ). This parameter is determined from a triaxial compression test on a drained sample prepared as dense as possible, and typically tested at 100 kPa initial effective confining stress to give an estimate of the maximum dilatancy of the soil. The measured data is again processed into stress dilatancy form (ie  $\eta$  vs  $D$ ), and as at peak strength the incremental elastic strains are zero the parameter  $D^p$  can be read directly from this plot. The CSL has already been determined (as described in Section 3.1), so the value of  $\psi$  at peak dilation can be computed from the corresponding mean effective stress and void ratio. Hence  $\chi$  follows immediately from the slope of the line through  $\eta$  vs  $D^p$  and the origin (see Figure 3-4). In practice it is preferable to test at least two dense samples to get some redundancy in the parameter estimate.

The final parameter of interest is the hardening modulus  $H$ . Hardening modulus is determined by formal modelling of experiments. Formal modelling is used because this provides the opportunity to optimize all the parameter estimates to test data.

$H$  is determined under conditions of fixed principal stress direction, a requirement met by the conventional triaxial test equipment. Drained tests are used, ideally with concurrent bender element measurements so that the elastic modulus is known. The calibration procedure used is to guess  $H$ , compute the entire stress strain behaviour, and compare the computed behaviour to that measured.  $H$  is then revised and the process repeated until a best-fit is obtained (see Figure 3-5). Once the best-fit for  $H$  has been obtained for each test, these values are reviewed to determine whether  $H$  should be considered a constant, or a function (often a linear function of initial  $\psi$ ). The fits for  $H$  are then re-evaluated for the proposed function and optimized over the available test data. Note that the objective of the calibration is to provide a ‘good’ fit over the range of tested pressures and states (or densities), not the best fit for a single test.

The NorSand equations of Table 2-1 are very easy to implement using a Euler scheme within the VBA environment of Excel, numerical integration being required because there are no closed form solutions to the equations. The spreadsheet corresponding to triaxial conditions for *NorSand-M* FISH Version 6 is available on the Itasca web site. All code is open source.

In evaluating  $H$  it is important to model tests over at least loose and dense states, since the available experience to date is that  $H$  depends on  $\psi$  (e.g. Figure 2-4). Thus the two drained tests used for the CSL determination are modelled, as well as the dense tests used to estimate  $\chi$ .

A weak point is the reliance on reconstituted samples, since there is no assurance at all that such reconstitution in any way replicates in situ fabric. To date, this issue has been approached by reconstituting samples using pluviated as well as moist tamped techniques, allowing the effect of fabric on  $H$  to be estimated. Of course this weakness is not specific to NorSand, all models using laboratory calibrations have to face the same issue of the relevance of laboratory samples to actual in situ conditions. It may prove possible to determine  $H$  in situ using the self-bored pressuremeter (Shuttle, 2006), but further work is needed in this area.

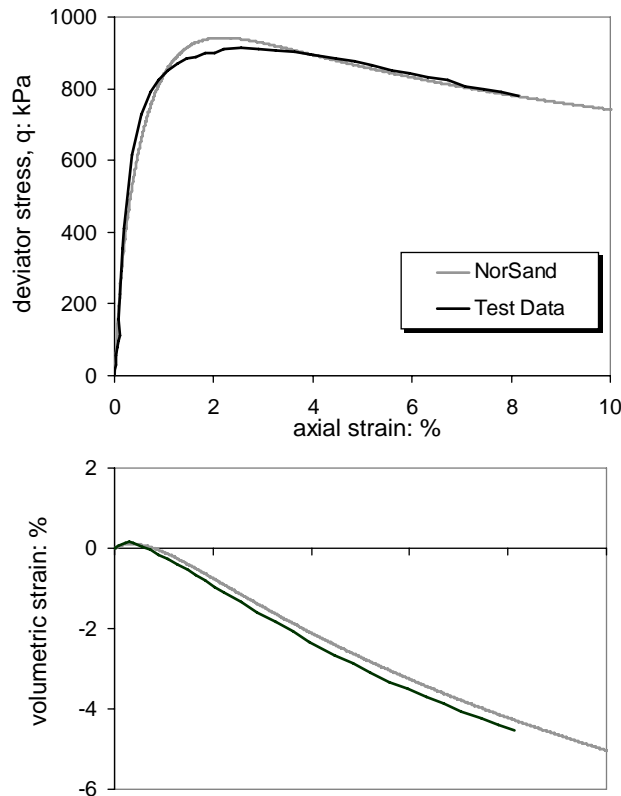


Figure 3-5 Example triaxial calibration to determine H

### 3.4 Measuring state

A central question in NorSand, or any other state parameter based model, is determining the soil's  $\psi$ . For laboratory testing the  $\psi$  throughout the test can be deduced from the known pressure and void ratio, once the critical state locus has been determined. Analysis may be used to determine an acceptable range of  $\psi$  in situ. But determining the actual in situ  $\psi$  is more difficult. In virtually all cases this will require in situ testing rather than trying to recover undisturbed samples, although sometimes with more silty to clay samples careful logging of water content can be a substantial help.

The methodology to determine  $\psi$  in situ is primarily based on the cone penetration test (CPT), a test that provides both excellent repeatability, accuracy, and a continuous profile. Initially, work concentrated on calibration chamber data. The calibration chamber is essentially a large triaxial cell, typically about 1.2 m in diameter. Sand is carefully placed at constant and known density, and the desired stress regime applied with vertical and radial stresses independently controlled. The CPT is pushed into the sand in the calibration chamber, just as in the field, with CPT data recorded in the usual way. Testing over a range of densities and applying a range of confining stress levels develops a map between CPT penetration resistance  $q_c$ , initial confining stress, geostatic stress ratio, and state (or relative density). However, because setting up a sample of sand in adequately sized calibration chambers is not a trivial undertaking (over 2 tons of sand is involved) the number of such programs is small.

Fifteen years ago, systematic evaluation of the then available data from calibration chamber tests on the CPT allowed the CPT data to be expressed in terms of  $\psi$ . The results were reported in two papers (Been et al, 1986, 1987a) and showed that the CPT responded to soil state according to the simple equation:

$$Q = \frac{3}{1 + 2K_0} k \exp(-m\psi) \quad (3)$$

where  $k$ ,  $m$  are two soil specific coefficients,  $K_0$  is the geostatic stress ratio, and the dimensionless CPT resistance is  $Q = (q_t - \sigma_v) / \bar{\sigma}_v$ . In practice the  $(3/(1+2K_0))$  term is usually set to unity for simplicity.

Been et al (1986, 1987a) contained data on seven sands: Ottawa sand, Reid Bedford sand, Hilton mines tailings, Monterey no.1 sand, Ticino sand, Hokksund sand and Toyoura sand. Since the two Been et al. papers were published, additional chamber testing has produced data on seven more sands: Erskak (Been et al., 1987b), Syncrude Tailings (Golder Associates, 1987), Yatesville silty sand (Brandon et al., 1990), Chep Lap Kok and West Kowloon (Golder Associates 1996), and Da Nang (Hsu, 1999). The data from these additional sands continue to show the same trends.

Although the equation relating CPT resistance and  $\psi$  is simple and consistent with a proper dimensionless approach, it was criticized on the grounds that careful examination of the reference chamber test data indicated significant bias with stress level (Sladen, 1988, 1989). In terms of the uncertainty introduced by neglecting stress level, Sladen substantially exaggerated the bias but that does not affect the fact that the Been et al methodology has an uncertainty of  $|\Delta\psi| < 0.05$  across the stress range considered because of stress level effects.

The existence of a stress level bias in (3) is curious given the dimensionless formulation. Shuttle & Jefferies (1998) used NorSand in a finite element analysis of cavity expansion to directly address the stress level effect postulated by Sladen. The detailed numerical simulations showed that (3) was an accurate representation of the relation between penetration resistance and state, as shown on Figure 3-6 for Ticino sand. The stress level bias was caused by treating  $k$ ,  $m$  as constants. These parameters should be functions of  $G/\bar{\sigma}_m$  but which was neglected in the work of Been et al.

Returning to the practical. Equation (3) is useful, but none but the largest projects can afford chamber testing to determine the parameters  $k$  and  $m$ . So, how to get these properties? Extensive numerical simulations using NorSand (Shuttle & Jefferies, 1998) produced relations for  $k$ ,  $m$  in terms of the soil's properties, and fitting trend lines to the numerical results gave:

$$k = (f_1(I_r) f_2(M) f_3(N) f_4(H) f_5(\lambda) f_6(v))^{1.45} \quad (4)$$

$$m = 1.45 f_7(I_r) f_8(M) f_9(N) f_{10}(H) f_{11}(\lambda) f_{12}(v) \quad (5)$$

where the fitted functions  $f_1 - f_{12}$  are simple algebraic expressions given in Table 3-1. Note that of the twelve parameters used to define  $k$  and  $m$ , all but two are constants for a given soil. Only  $f_1$  and  $f_7$ , which are functions of the stress level, vary spatially within the soil.

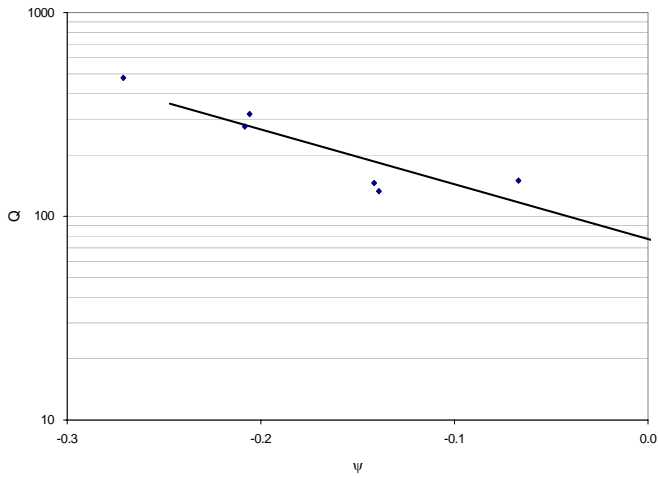
The performance of the approximate inversion was verified by taking 10 sets of randomly generated soil properties/states and computing the  $Q$  value using the full numerical procedure. This computed  $Q$  was then input into the inversion to recover the estimated value of  $\psi$ . The inversion recovers  $\psi$  with an accuracy of  $\pm 0.02$ . These numerical simulations were made using an earlier version of NorSand, but as the parameter definitions remain unchanged the approximate inversion should remain valid.

Table 3-1 Approximate expressions for general inverse form  $\psi=f(Q)$

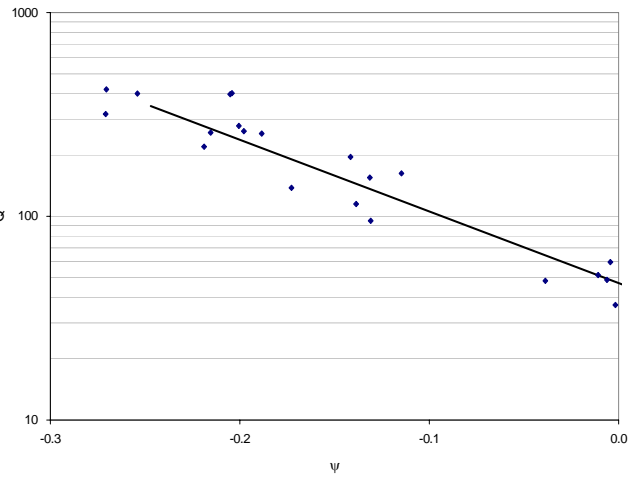
<i>Function</i>	<i>Approximation</i>
$f_1(G/p_0)$	$3.79 + 1.12 \ln(G/p')$
$f_2(M)$	$1 + 1.06 (M_{tc} - 1.25)$
$f_3(N)$	$1 - 0.30 (N - 0.2)$
$f_4(H)$	$(H / 100)^{0.326}$
$f_5(\lambda)$	$1 - 1.55 (\lambda - 0.01)$
$f_6(\nu)$	Unity
$f_7(G/p_0)$	$1.04 + 0.46 \ln(G/p')$
$f_8(M)$	$1 - 0.40 (M - 1.25)$
$f_9(N)$	$1 - 0.30 (N - 0.2)$
$f_{10}(H)$	$(H / 100)^{0.15}$
$f_{11}(\lambda)$	$1 - 2.21 (\lambda - 0.01)$
$f_{12}(\nu)$	Unity

The approximate inversion to determine  $\psi$  from CPT data is readily used in practical situations by adopting a seismic CPT for at least some of the soundings. The seismic CPT allows  $G$  to be determined from shear wave velocity measurements using the straightforward polarity reversal method. It is not onerous to do, and has small cost impact on a site investigation.

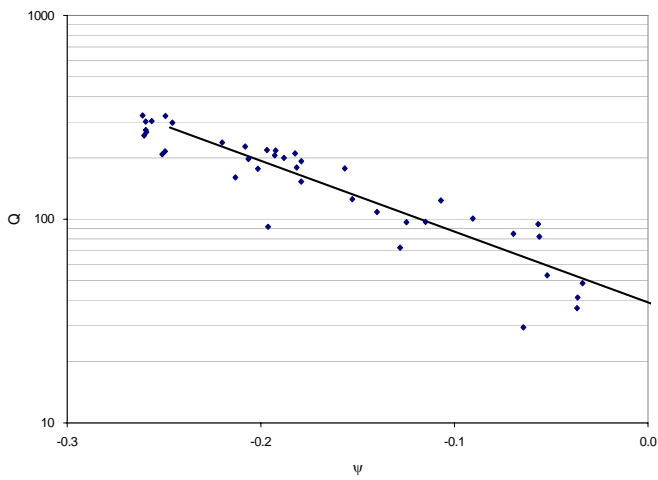
A difficulty arises at the moment when dealing with silts. These soils are very prone to disturbance, like sands. And even if sampled are often too soft to be set-up in a triaxial test without collapsing under their self-weight. However, CPT soundings in such soils are usually not drained and the excess pore pressures prevent the application of (3) – (5) to determine  $\psi$  in situ. Further work is required to establish a proper methodology to estimated  $\psi$  in silts, although a first order empirical approach has been suggested by Plewes et al (1992).



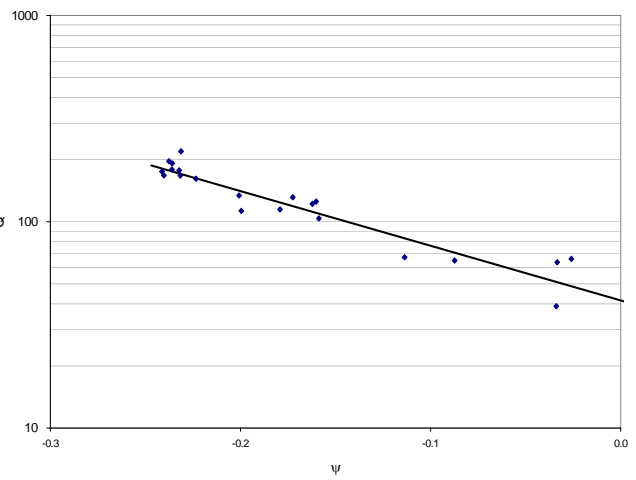
(a)  $25 < p' < 30$  kPa



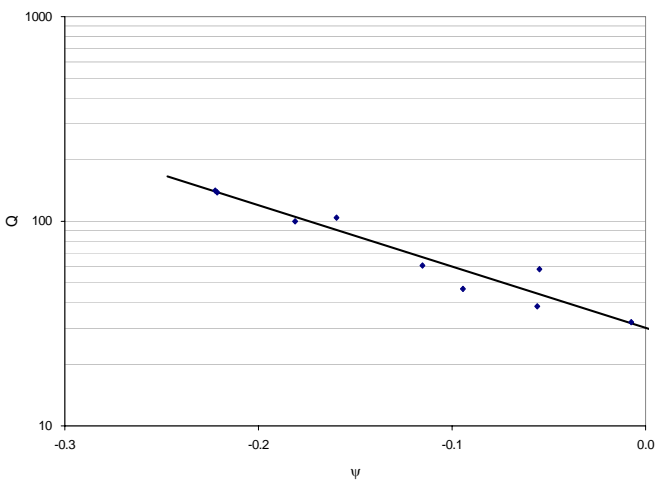
(b)  $37 < p' < 47$  kPa



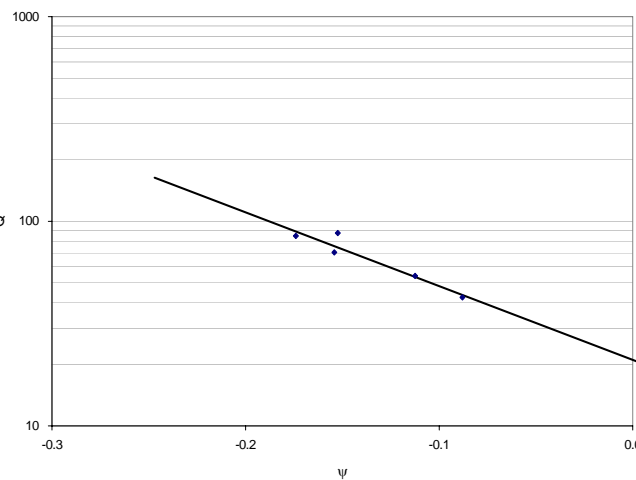
(c)  $65 < p' < 85$  kPa



(d)  $185 < p' < 240$  kPa



(e)  $300 < p' < 370$  kPa



(f)  $440 < p' < 460$  kPa

Figure 3-6 Comparison of CPT resistance in Ticino Sand with trendlines from numerical simulations using finite element implementation of NorSand

### 3.5 Testing range

Although it is common for laboratory testing to focus on preparing samples with conditions as close as possible to those found in situ, such an approach is misguided for models like NorSand. Testing for models that predict the effect of density and stress level on soil behaviour should be targeted to cover the extremes of possible void ratios to the extent that it can be practically done. It is somewhat less important to target a wide range of stresses, but a range of initial confining stress of 50 kPa to 500 kPa should be sought. The goal is to get the end-member behaviour as that provides the greatest opportunity to discern any limitations of the model in representing the soil of interest, and also operates the model in an interpolation, rather than an extrapolation, mode.

Table 3-2 presents some example parameters sets for NorSand properties of various soils, as well as the reference where the details of the calibration can be found. Three of the soils shown in the table are standard laboratory quartz sands, one (Erksak) is a construction sand that is a hard quartz material but which contains about 1% silt. The Bennett silty sand is almost the exact opposite of these laboratory sands, being a well graded material used to construct the core of a large dam. Bonnie Silt is the silt used in the VELACS tests. Bothekennar Clay is the soil from the UK's soft-soil research site. In all cases NorSand provided an excellent representation of the test data.

Table 3-2 Some Examples of Calibrated Soil Property Sets for NorSand

Soil	CSL			Plasticity			Elasticity	
	$\Gamma$	$\lambda_e$	$M_{tc}$	$N$	$H$	$\chi$	$I_r$	$\nu$
Erksak Sand <sup>2</sup>	.817	.014	1.26	0.3 <sup>1</sup>	Pluviated: 70 – 1400 $\psi$ Moist tamped: 130–1400 $\psi$	4.1	150 - 1000	0.2
Ticino Sand <sup>3</sup>	0.962	0.0248	1.23	0.3 <sup>1</sup>	115–420 $\psi$	3.5	300 - 500	0.2
Hilton Mines <sup>2</sup>	1.315	0.0738	1.39	0.3 <sup>1</sup>	65	3.5	300 - 500	0.2
Brasted Sand <sup>3</sup>	0.902	0.02	1.27	0.3 <sup>1</sup>	50–1125 $\psi$	2.8	500	0.2
Nevada Sand <sup>4</sup>	0.910	0.02	1.20	0.3 <sup>1</sup>	100–300 $\psi$	3.5	175	0.2
Bennett silty sand <sup>5</sup>	0.45	0.018	1.40	0.3 <sup>1</sup>	100 - 150	3.5	300 - 500	
Bonnie Silt <sup>6</sup>	1.10	0.07	1.32	0.3 <sup>1</sup>	20 - 45	3.8	40 - 80	
Bothkennar Clay <sup>7</sup>	2.76	0.181	1.83	0.3 <sup>1</sup>	300	3.5	36.6	
Da Nang <sup>8</sup>	0.99	0.0317	1.25	0.35	40-220 $\psi_0$	4.3	300-2000 $\psi_0$	0.2
							From fitting to triaxial data	
Hokksund <sup>8</sup>	0.934	0.0235	1.00	0.40	138+513 $\psi_0$ + 2250 $\psi_0^2$	4.0	$\frac{720}{e^{1.30}} \times \left(\frac{p'}{p_a}\right)^{0.46} \times p_a / p'$	0.2
							After Lo Presti et al. (1992)	
Ottawa <sup>8</sup>	0.754	0.0122	1.24	0.45	180-400 $\psi_0$	4.0	$\left(\frac{2.66 + e}{1 + e}\right) \times (381 - 259e)^2$ $\times \left(\frac{p'}{p_a}\right)^{0.52} / p'$	0.2
							After Robertson et al. (1995)	
Syncrude <sup>8</sup> , Oil Tailings	0.890	0.0283	1.27	0.28	43-296 $\psi_0$ + 1296 $\psi_0^2$	5.8	$\left(\frac{2.64 + e}{1 + e}\right) \times (311 - 188e)^2$ $\times \left(\frac{p'}{p_a}\right)^{0.52} \times K_0^{0.26} / p'$	0.2
							After Cunning et al. (1995)	
Toyoura 160 <sup>8</sup>	0.983	0.019	1.28	0.41	100	4.4	$18.35 \times 10^6 \times \frac{(2.17 - e)^2}{1 + e}$ $\times p'^{-0.47}$	0.2
							After Chaudhary et al. (2004)	

<sup>1</sup> Value of N assumed, not measured

<sup>2</sup> Jefferies and Shuttle (2005)

<sup>3</sup> Shuttle and Jefferies (1998)

<sup>4</sup> Been et al. (1993)

<sup>5</sup> Shuttle and Jefferies (2000)

<sup>6</sup> Vyazmensky (2004)

<sup>7</sup> Shuttle (2003)

<sup>8</sup> Ghafghazi and Shuttle (2008a)

## 4. FISH EXAMPLES

### 4.1 Plane strain element test

This example models a drained plane strain element test on a dense sand (see Figure 4-1). The cell pressure was 200 kPa, with  $K_0$  equal to 0.95. The material properties of the sand are given in Table 4-1. The input file is titled plane.dat.

Table 4-1 NorSand Soil Properties for Example 'Plane'

<i>Property</i>	<i>FISH Name</i>	<i>Value</i>
$\Gamma$	m_Gamma	0.816
$\lambda_e$	m_Lambda	0.014
$M_{tc}$	m_M	1.26
$N$	m_N	0.35
$H$	m_H	700.
$\chi_{tc}$	m_chi	4.0
$G$	m_G	2.5e5
$\nu$	m_nu	0.2
$R$	m_OCR	1.0
$\psi$	m_psi	-0.2

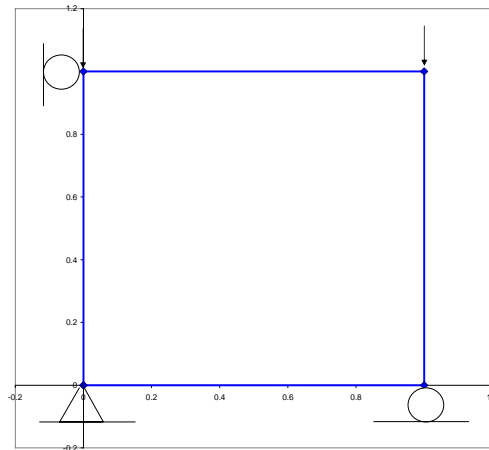


Figure 4-1 Geometry, boundary and loading conditions for Plane.dat

The tracked outputs for the simulation are described in Table 4-2. The results of the simulation are plotted in Figure 4-2. Also shown on Figure 4-2 are the results from an independent solution - a direct integration solution coded within Excel using the Visual Basic Application (VBA) compiler. The match between the direct integration and FISH-FLAC solution is excellent.

Table 4-2 Tracked outputs for Plane.dat

<b>History</b>	<b>Name</b>	<b>Description</b>
1	ydisp i=1 j=2	Displacement at loaded node (top of sample) (m)
2	m_p i=1 j=1	Mean effective stress (kPa)
3	m_q i=1 j=1	Deviatoric stress invariant (kPa)
4	m_void i=1 j=1	Void ratio (-)
5	m_sxx i=1 j=1	Effective stress, x-direction (kPa)
6	m_syy i=1 j=1	Effective stress, y-direction (kPa)
7	m_szz i=1 j=1	Effective stress, z-direction (kPa)
8	m_sxy i=1 j=1	Effective stress, shear in xy (kPa)
9	m_Lode i=1 j=1	Lode angle (in radians)
10	m_e i=1 j=1	Volumetric strain (-)
11	Unbal	Unbalanced force

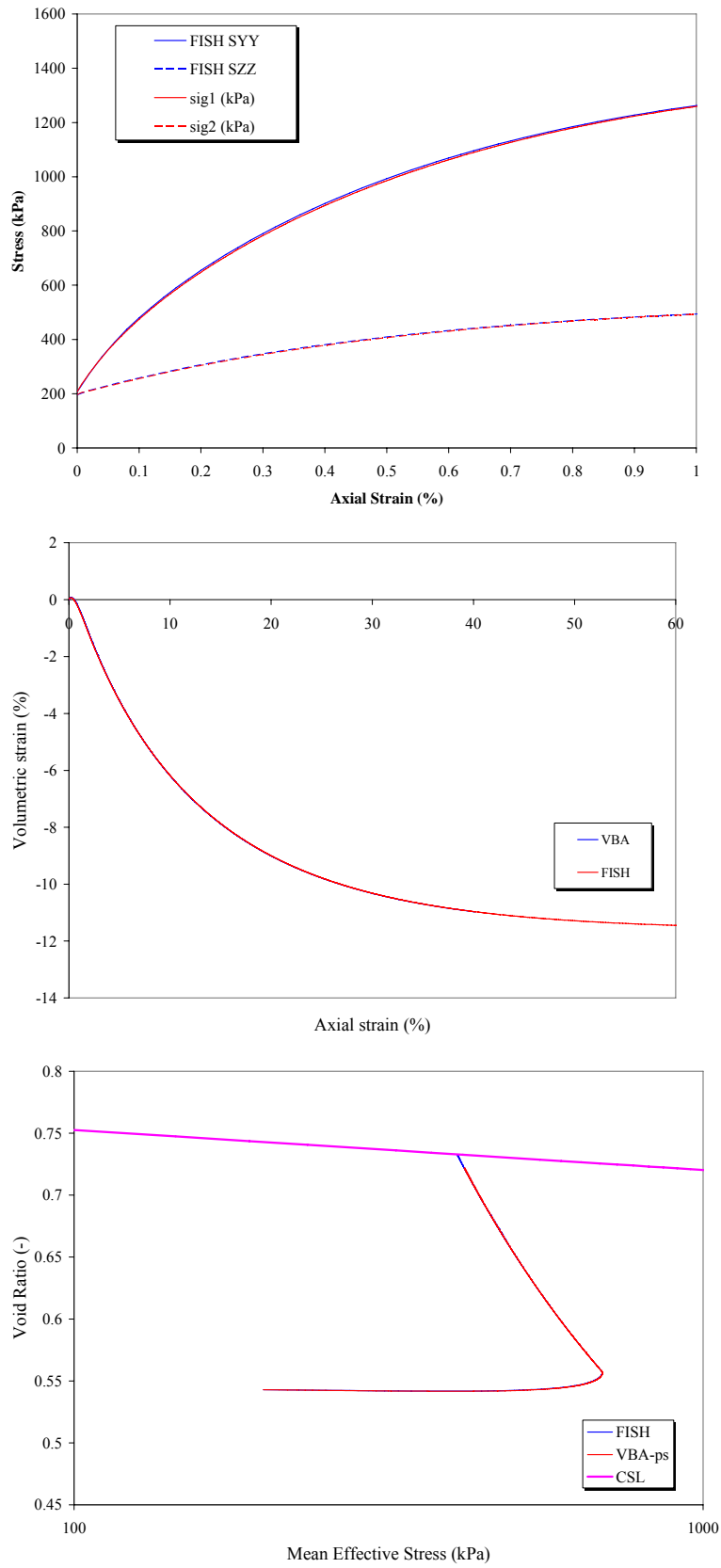


Figure 4-2 Results from plane.dat compared against the direct integration VBA solution

## 4.2 Passive wall

The second example is a passive wall, showing the effect of varying initial state parameter on the load-displacement behaviour of the wall. This example uses a coarse mesh discretization (see Figure 4-3) and is for illustrative purposes only – a FLAC simulation of a real wall requires a much finer mesh to achieve an accurate solution (but would, of course, run more slowly). The input files are titled ‘NS\_Rwall\_XYZ.dat’ where X is ‘p’ for +, ‘m’ for -, and YZ are the digits after the decimal place in the initial state parameter.

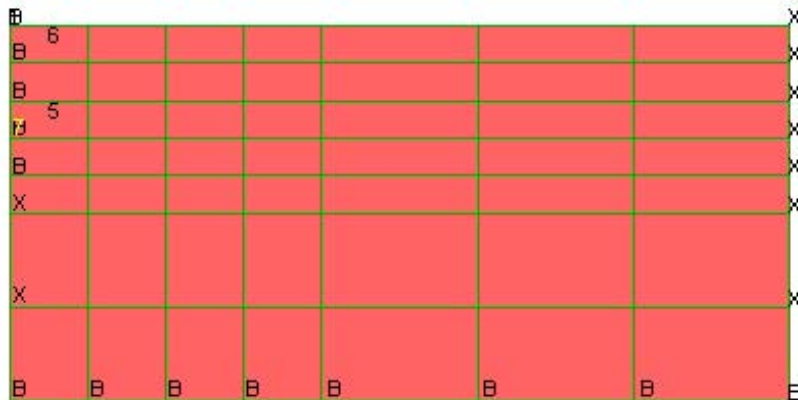


Figure 4-3 Mesh used for passive wall

The 7 by 7 mesh has dimensions of 4m depth and 10m width. The rough wall is 2m in height, and the NorSand properties of the soil are given in Table 4-3. The initial state parameter,  $\psi_0$ , varies over the full practical range from very dense ( $\psi_0 = -0.3$ ) to very loose ( $\psi_0 = 0.1$ ). The displacement is applied as a “ramp loading” increasing to  $10^{-5}$  over 40,000 steps. The tracked outputs from the simulation are given in Table 4-4.

Table 4-3 NorSand Soil Properties for Example 'Rough Wall'

<i>Property</i>	<i>FISH Name</i>	<i>Value</i>
$\Gamma$	m_Gamma	0.754
$\lambda_e$	m_Lambda	0.0122
$M_{tc}$	m_M	1.24
$N$	m_N	0.45
$H$	m_H	300
$\chi_{tc}$	m_chi	3.00
$G$	m_G	8.5e7
$\nu$	m_nu	0.2
$R$	m_OCR	1.0
$\rho$	dens	1937
$\psi_0$	m_psi	-0.3, -0.2, -0.1, 0.0, 0.1

Table 4-4 Tracked outputs for the rough wall

History	Name	Description
1	xdis i=1 j=8	Displacement of wall (m)
2	Unbal	Unbalanced force
3	Pav1	Force on the wall, calculated from xforce
4	Pav2	Force on the wall, calculated from horizontal stress
5	m_sxx i=1 j=5	Effective stress in front of wall, x-direction (kPa)
6	m_sxx i=1 j=7	Effective stress in front of wall, x-direction (kPa)
7	xvel i=1, j=5	Velocity of the wall (m/step)

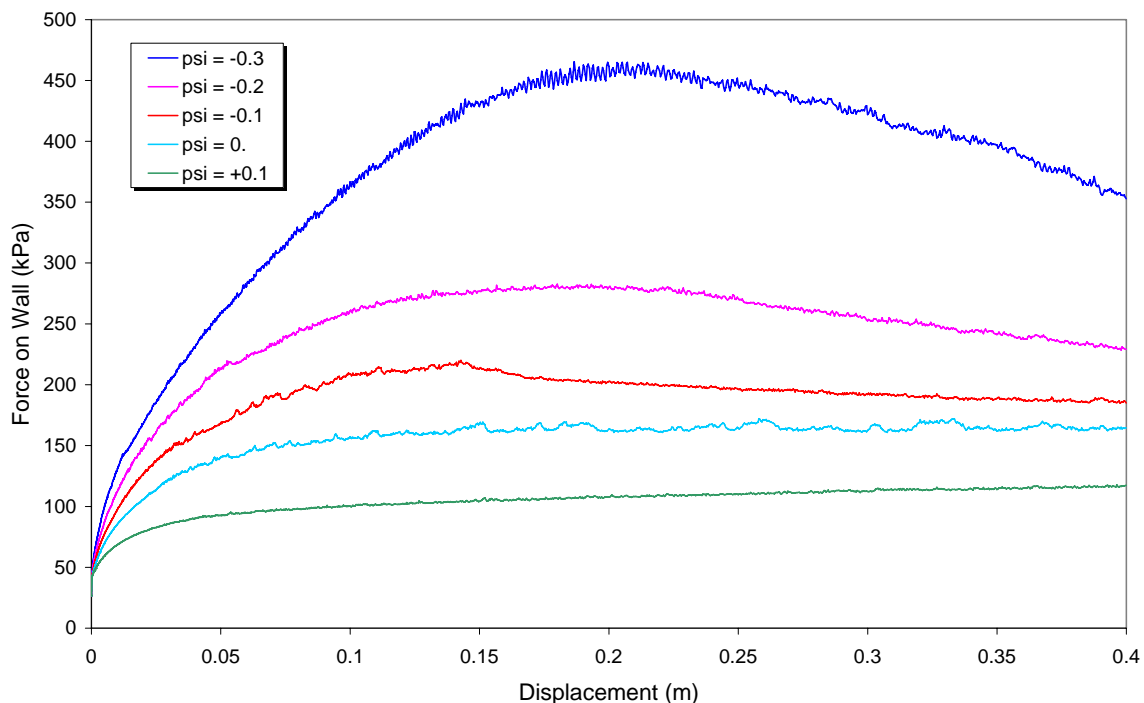


Figure 4-4 Effect of initial state on the lateral force of a 2m high rough wall

The results of the analyses are given in Figure 4-4 as the force against the wall (from xforce at the loaded nodes) versus wall displacement. The effect of initial void ratio is clearly indicated, with strain softening observed for the denser, negative initial states.

The free boundary at the surface of the soil is unstressed in this problem. It is worth noting that NorSand is undefined for tensile mean effective stresses – and fails under this condition – so problems where low mean effective stresses are likely require loading with small velocities to prevent ‘drift’ allowing a tensile mean effective stress to occur.

## 5. REFERENCES

- ASCE (2010) Geo-Institute of the American Society of Civil Engineers Compaction Grouting Consensus Guide, ASCE/G-I 53-10 (ed. D.A. Shuttle): ISBN: 978-0-7844-1094-3
- Been K., Crooks J.H.A., Becker D.E. and Jefferies M.G. (1986). "The cone penetration test in sands: Part I, state parameter interpretation", *Geotechnique* 36, 239-249.
- Been K., Jefferies M.G., Crooks J.H.A. and Rothenberg L. (1987a). "The cone penetration test in sands: Part II, general inference of state", *Geotechnique*, 37, 285-299.
- Been K., Lingnau, B.E., Crooks J.H.A. and Leach, B.. (1987b) "Cone penetration test calibration of Erksak (Beaufort Sea) sand", *Can. Geot. J.* 24, 601-610.
- Been, K., Jefferies, M.G., Hachey, J.E. & Rothenburg, L. (1993); Numerical prediction for Model No 2. In *Verification of Numerical Procedures for Analysis of Soil Liquefaction Problems* (Arulanandan & Scott, eds), 331-341. Balkema.
- Brandon, T.L., Clough, G.W. and Rajardjo, R.P. (1990). "Evaluation of liquefaction potential of silty sands based on cone penetration resistance", Research Report to National Science Foundation, Grant ECE-8614516, Virginia Polytechnic Institute.
- Dabeet, A. and D.A.Shuttle (2008) "Deformation characteristics of sands in unloading", 61st Canadian Geotechnical Conference and 9th Joint CGS/IAH-CNC Groundwater Conference Edmonton, September 21-24, 2008.
- Ghafghazi, M., and D.A. Shuttle (2008a) "Interpretation of Sand State from CPT Tip Resistance". *Géotechnique*, 58, no. 8, pp. 623-634.
- Ghafghazi, M., and D.A. Shuttle (2008b) "Evaluation of Soil State from SBP and CPT: A Case History". *Canadian Geotechnical Journal*, 45, pp 824-844.
- Golder Associates (1987). "Cone penetrometer calibration chamber tests on Syncrude Tailings", *Project report 872-2402* to Syncrude Canada Limited.
- Golder Associates (1996). "Review of Sand Fill Characterization Study", *Project Report 9452-1095* to Hong Kong University of Science and Technology.
- Hsu, H. H. (1999). Cone Penetration Tests in Sand under Simulated Field Conditions. PhD thesis, National Chiao Tung University, Hsin Chu, Taiwan.
- Jefferies, M.G. (1993). "NorSand: a simple critical state model for sand", *Geotechnique* 43, 91-103.
- Jefferies, M.G. (1997). "Plastic work and isotropic softening in unloading", *Geotechnique*, 47, 1037-1042.
- Jefferies, M.G. & Been, K. (2000). "Implications for critical state theory from isotropic compression of sand", *Geotechnique* 50, 419-429.
- Jefferies, M.G. and Shuttle, D.A. (2002). "Dilatancy In General Cambridge-Type Models", *Geotechnique* 52, 625-638.
- Jefferies, M.G. and D.A. Shuttle (2002) "Discussion: The Effect Of The Development Of Undrained Pore Pressure On The Efficiency Of Compaction Grouting", *Géotechnique*, Vol. 52, No. 1, pp 74-75.
- Jefferies, M.G. and D.A. Shuttle (2005) "NorSand: Features, Calibration and Use". Invited paper for the ASCE Geo-Institute Geo-Frontiers Conference, Austin, Texas, January 24-26, 2005. Published as Geotechnical Special Publication No. 128, Soil

- Constitutive Models: Evaluation, Selection, and Calibration, pp 204-236, editors Jerry A. Yamamuro and Victor N. Kaliakin.
- Jefferies, M.G. & Been, K. (2006) "Soil Liquefaction: A critical state approach", Taylor and Francis, Abingdon.
- Jefferies, M.G. and D.A. Shuttle (2010) "On the Operating Critical Friction Ratio in General Stress States", *Géotechnique* (in press).
- Matsuoka, H. & Nakai, T. (1974). "Stress-deformation and strength characteristics of soil under three different principal stresses", *Trans. JSCE* 6, 108-109.
- Nova, R. (1982). "A constitutive model under monotonic and cyclic loading", in *Soil Mechanics – Transient and Cyclic Loads* (eds Pande & Zienkiewicz), 343-373. Wiley.
- Parry, R.H.G (1956) "On the yielding of soil: Correspondence", *Géotechnique* 8(4), 183-186.
- Plewes, H.D., Davies, M.P., and Jefferies, M.G. (1992); CPT based screening procedure for evaluating liquefaction susceptibility. *Proc 45th Can. Geot. Conf.*, Toronto
- Resende, L. & Martin, J.B. (1985). "Formulation of Drucker-Prager Cap Model", *ASCE J. Eng Mech* 111, 855-881.
- Roscoe, K.H. and Burland, J.B. (1968). "On the generalized stress-strain behaviour of 'wet' clay". In *Engineering plasticity* (eds. J. Heyman and F.A. Leckie) pp. 535-609. Cambridge University Press.
- Rousé, P.C., D.A. Shuttle, and R.J. Fannin (2006) "Implementation of Critical State Models within FLAC", *Proceedings of the 4th International FLAC Symposium on Numerical Modelling in Geomechanics - 2006*, 29-31 May, Madrid, Spain, pp 379-385.
- Schofield, A. & Wroth, C.P. (1968). *Critical State Soil Mechanics*. McGraw-Hill.
- Sladen, J.A. (1988); Discussion: Cone penetration test calibration for Erksak sand. *Can. Geotech. J* 26, 173-177.
- Sladen J.A. (1989); Problems with interpretation of sand state from cone penetration test. *Géotechnique* 39, 323-332.
- Sladen, J.A. & Handford, G. (1987). "A potential systematic error in the laboratory testing of very loose sands", *Can. Geotech. J.* 24, 462-466.
- Shuttle, D.A. & Jefferies, M.G. (1998); "Dimensionless and unbiased CPT interpretation in sand". *IJNAMG* 22, 351-391.
- Shuttle, D.A. and M.G. Jefferies (2000) "Prediction and Validation of Compaction Grout Effectiveness", *ASCE Geotechnical Special Publication 104*, *Advances in Grouting and Ground Modification*, (eds Krizek & Sharp).
- Shuttle, D.A. (2003) "Effect Of Pore Pressure Dissipation On SBP Tests In Clay" *Proc. 56th Can. Geotech. Conf.*, Winnipeg.
- Shuttle, D.A. (2006) "Can the Effect of Sand Fabric on Plastic Hardening be Determined Using a Self-Bored Pressuremeter?". *Canadian Geotechnical Journal*, 43, pp 659-673.
- Shuttle, D.A. and J. Cunning (2007) "Liquefaction Potential of Silts from CPTu", *Canadian Geotechnical Journal*, 44, pp 1-19.
- Shuttle, D.A. and J. Cunning (2008) "Discussion: Liquefaction Potential of Silts from CPTu", *Canadian Geotechnical Journal*, 45, pp 142-145.

- Verdugo, R. (1992). Discussion on 'The critical state of sand'. *Géotechnique* 42, p655-658.
- Vyazmensky, A. (2004). "Numerical modelling of time dependent pore pressure response induced by helical pile installation", M.A.Sc. Thesis, University of British Columbia.
- Vyazmensky, A.M., D.A. Shuttle and J.A. Howie (2004) "Coupled Modelling Of Observed Pore Pressure Dissipation After Helical Pile Installation", Proceeding of the 57th Canadian Geotechnical Society Conference, Quebec, 25-27, October 2004 . (6 pages)